Preprint PFC/JA-81-32

RIPPLED-FIELD MAGNETRON

G. Bekefi

December 1981

RIPPLED-FIELD MAGNETRON

G. Bekefi

Department of Physics and Research Laboratory of Electronics

Massachusetts Institute of Technology

Cambridge, Massachusetts 02139

ABSTRACT

The rippled-field magnetron is a novel crossed-field millimeter wave source in which electrons move under the combined action of a radial electric field, an axial magnetic field and an azimuthally periodic wiggler magnetic field, $\vec{B}_w \cos(N\theta)$ oriented transversely to the flow. Estimates are given of the frequency and growth rate of the free electron laser (FEL) type of instability excited in this smooth-bore magnetron configuration.

To achieve efficient conversion of energy from a stream of free electrons to electromagnetic radiation, near synchronism must be attained between the velocity of the electrons and the phase velocity of the wave. In crossed-field devices,[1] of which the magnetron is a typical example, this synchronism occurs between electrons undergoing a $\vec{v}=\vec{E}_0\times\vec{B}_0$ drift in orthogonal electric and magnetic fields, and an electromagnetic wave whose velocity is reduced by a slow wave structure comprised of a periodic assembly of resonant cavities. This complex system of closely spaced resonators embedded in the anode block limits the conventional magnetron to wavelengths in the centimeter range. Moreover, at high power outputs typical of relativistic magnetrons,[2] rf or dc breakdown in the electron-beam interaction space, and at the sharp resonator edges poses serious problems. The rippled-field magnetron is a novel source of coherent radiation devoid of physical slow-wave structures. Thus, the configuration of the anode and cathode is similar to the so-called "smooth-bore" magnetron.[3] However, it differs from the smooth bore magnetron in that the electrons are subjected to an additional field, an azimuthally periodic (wiggler) magnetic field $\vec{B}_w$ oriented transversely to the flow velocity $\vec{v}$. The resulting $-e\vec{v}\times\vec{B}_w$ force gives the electrons an undulatory motion which effectively increases their velocity,[4] and allows them to become synchronous with one of the fast TE or TM electromagnetic modes (phase velocity $\geq c$) characteristic of the smooth-bore magnetron. We note that this technique is also the basis of free-electron lasers[5] (FEL). Thus, in the rippled-field magnetron, the steady state electron motions are governed by well-known magnetron equilibria, but the

high frequency wave instability which leads to the sought-for radiation is determined by an FEL-like interaction. The device differs from the FEL in that the electron source (the cathode) and the acceleration region (the anode-cathode gap) are an integral part of the rf interaction space. This makes for high space-charge densities and for large growth rates of the FEL instability. Typically, the magnetron configuration is cylindrical rather than linear as in conventional FEL's, and the system is therefore very compact. The cylindrical geometry also allows for a continuous circulation of the growing electromagnetic wave and thus the system provides its own internal feedback. Therefore, the rippled-field magnetron is basically an oscillator rather than an amplifier as is the case of the FEL.

The device is illustrated schematically in Fig. 1. It comprises a smooth cylindrical anode of radius r_a enclosing a smooth coaxial cylindrical cathode of radius r_c. The electrons, emitted by the cathode either thermionically or by field emission[2,3] from a cold metal surface, are subjected simultaneously to two steady, or quasi-steady fields acting at right angles to one another: a uniform, axial magnetic field B_{0z} produced by say a solenoid, and a radial electric field $E_{0r}(r)$ generated by applying a voltage V between the electrodes. As a result, a space charge cloud forms, partially filling the interaction gap (r_a-r_c); the electrons undergo azimuthal rotation having a sheared, radially dependent velocity $v_\theta=E_{0r}(r)/B_{0z}$. To achieve this "Brillouin flow equilibrium", the voltage V must be turned on slowly[6] on a time scale long compared with the cyclotron period; and the strength of the magnetic field must exceed the critical field[6,7]

$$B_{0c} = (m_0 c/ed_e)(\gamma_0^2 - 1)^{1/2} \qquad (1)$$

where e and m_0 are the electron charge and rest mass, respectively, $\gamma_0 = 1 + (eV/m_0c^2)$ and $d_e \equiv (r_a^2 - r_c^2)/2r_a$ is the effective anode-cathode gap width. Superimposed on the $\vec{E}$ and $\vec{B}$ fields is an azimuthally periodic magnetic (wiggler) field of the form $\vec{B}_w \cos(N\theta)$ where $|\vec{B}_w|$ is the amplitude of the field and $N = 2\pi r_c/\ell$ the number of spatial periods. In Fig. 1 the wiggler field is primarily in the radial direction and could be generated, for example, by samarium-cobalt bar magnets[8] embedded in the anode and cathode blocks (but protected from the electron stream by the smooth, non-magnetic metal electrodes). The resulting periodic force acting on the electrons is along the $\pm z$ axis which is also the direction of polarization of the emitted radiation. Alternately one can envision a wiggler magnetic field oriented primarily along the z axis in which case the electrons experience a periodic radial force, with the result that the ensuing radiation will also be radially polarized.

When the anode-cathode gap $d = (r_a - r_c)$ is small compared with the anode radius r_a, it is possible to approximate the cylindrical device by a planar analogue which is illustrated in Fig. 2. In this case, a fully relativistic analysis[7] of the Brillouin flow equilibrium and of the small amplitude wave[9] perturbations of the flow has been worked out in the absence of the wiggler magnetic field $\vec{B}_w$. One finds that when B_{0z} exceeds B_{0c} given by Eq. (1), an electron space charge partially fills the anode-cathode gap d to a thickness $x = x^*$ determined by the simultaneous solution of the equations

$$\gamma_0 \cosh(\alpha x^*) = 1 + A \sinh(\alpha x^*) \tag{2}$$

$$\alpha(d-x^*) = (1 + A^2 - \gamma_0^2)^{1/2} \tag{3}$$

where $A=eB_{0z}d/m_0c$ and $\gamma_0=1+eV/m_0c^2$. The constant α, likewise obtained from solving Eqs. (2) and (3), specifies the remaining parameters of the equilibrium flow, namely the electron velocity and density distributions $v_y(x)=c\tanh(\alpha x)$, $n(x)=(m_0c^2\varepsilon_0/e^2)\alpha^2\cosh(\alpha x)$, and the self-consistent electric and magnetic fields in the sheath, $E_x(x)=\alpha(m_0c^2/e)\sinh(\alpha x)$ and $B_z(x)=\alpha(m_0c/e)\cosh(\alpha x)$. We note that at every position $x\leq x^*$ the nonrelativistic plasma frequency $\omega_p = (ne^2/m_0\varepsilon_0)^{1/2}$ and the nonrelativistic cyclotron frequency $\Omega = (eB_z/m_0)$ are related through $\omega_p(x)=\Omega(x)/\gamma^{1/2}(x)$, where $\gamma(x) = \cosh(\alpha x)$. Thus ω_p and Ω are of the same order of magnitude, and at large operating magnetic fields $B_{0z} \gtrsim 10\text{kG}$, $\Omega \gtrsim 10^{11}\text{sec}^{-1}$. Hence the plasma frequency can be large which is important in achieving large levels of electromagnetic radiation.

Superposed on the Brillouin flow are slow (quasi-electrostatic) space-charge waves propagating along the y axis. Their dispersion characteristics have been studied extensively both for nonrelativistic[6,10,11] and relativistic[9] flows. Of particular interest is a class of short wavelength surface waves associated with a resonant interaction occurring with electrons that reside at or near the surface of the space-charge, $x\approx x^*$. For these waves the real part of the dispersion equation is given by[6,9]

$$\begin{aligned}\omega_r &\approx k v_y(x=x^*) \qquad (kc >> \Omega)\\ &= kc\tanh(\alpha x^*)\end{aligned} \tag{4}$$

Here ω_r is the real part of the complex frequency ω and k the real wave number; and α and x^* are determined from Eqs. (2) and (3).

The waves are unstable (ω has an imaginary part) and they grow in amplitude, drawing energy from the sheared velocity field of the Brillouin flow.[6,9]

In the presence of the wiggler field which has been ignored hitherto, the dispersion Eq. (4) takes on the form

$$\omega_r \simeq (k + k_0)c \tanh(\alpha x^*) \tag{5}$$

where $k_0=2\pi/\ell$ and ℓ is the period (see Fig. 2). As a result, the phase velocity of the wave ω_r/k is increased by a factor $1+(k_0/k)$. This enables the slow space charge wave to interact in phase synchronism with the (fast) electromagnetic wave that propagates in the anode-cathode gap. Setting $\omega\simeq kc$ for the electromagnetic wave (thereby neglecting effects due to the proximity of the electrode walls), and substituting for k in Eq. (5), yields the radiation frequency,

$$\omega \simeq k_0 c \tanh(\alpha x^*)[1 - \tanh(\alpha x^*)]^{-1}. \tag{6}$$

When the external axial magnetic field B_{0z} equals the critical field B_{0c} of Eq. (1), the electron space charge fills the entire gap and $x^*=d$. Now, $\tanh(\alpha d)=(\gamma_0^2-1)^{1/2}/\gamma_0$ and $\omega=\gamma_0^2 k_0 c\beta_0[1+\beta_0]$ where $\beta_0\equiv(1-(1/\gamma_0^2))^{1/2}$, which is the familiar result for the frequency of a free electron laser. As B_{0z} is increased relative to B_{0c}, the space charge thickness x^* shrinks, and $v_y(x=x^*)$ and the radiation frequency ω decrease. We can now compare the frequency given by Eq. (6) with the radiation frequency[7] $\omega\simeq k_0 c \tanh(\alpha x^*)$ of a conventional magnetron whose anode is pierced with a periodic assembly of resonators separated by a distance π/k_0. We see that for the same operating parameters (the same values of α and x^*), the rippled-field magnetron radiates at a higher frequency

than the conventional magnetron, and when $\tanh(\alpha x^*)$ approaches unity as is the case for relativistic velocities, the frequency enhancement over a conventional magnetron is very large.

The temporal growth rate of the wave amplitude can be estimated from the expression[5]

$$\omega_i = F^{1/4}[\gamma(x^*)^{1/2}\omega_p(x^*)/4\omega_r]^{1/2}\Omega_w \qquad (k_0 v_y > \Omega/\gamma) \quad (7)$$

applicable to FEL's operating in the high gain collective, Raman regime. Here ω_r is the radiation frequency given by Eq. (6), ω_i is the imaginary part of the complex frequency ω, $\Omega_w = eB_w/m_0$ is the nonrelativistic electron cyclotron frequency in a wiggler magnetic field of amplitude B_w, and $\omega_p(x^*) = [n(x=x^*)e^2/m_0\varepsilon_0]^{1/2}$ is the nonrelativistic plasma frequency of the resonant layer $x=x^*$. F is a phenomenological filling factor which describes the amplitude coupling of the electron stream to the electromagnetic wave. For a plane wave interacting with an infinitely wide electron stream of monoenergetic electrons, F is unity. For a sheared stream of electrons that is narrower than the electromagnetic beam, F is approximately given by the ratio of the beam area occupied by the resonant electrons at and near the sheath surface, to the electromagnetic beam area. Table 1 lists the computed characteristics of a rippled-field magnetron radiating at a wavelength of 1.3mm and operating at a voltage of 1022kV, an axial magnetic field B_{0z} = 10.32kG, and a wiggler field B_w=2.28kG, a value readily achieved[8] in the 0.5cm wide gap by use of samerium-cobalt bar magnets. The wiggler periodicity ℓ=1cm and the total number of periods N around the anode cylinder is 26. We see from Table 1 that the device is very compact. The value x^*/d has been chosen

arbitrarily to be approximately three quarters of the full gap width d=0.5cm. Thus, the computed radiation frequency ω_r is less than the maximum possible with given operating parameters. (The maximum value of ω_r obtained when $x^*=d$ equals $3.12\times10^{12}\,sec^{-1}$). The temporal growth rate was computed for the case of an ideal filling factor, F=1. The value $\omega_i=8.11\times10^{9}\,sec^{-1}$ corresponds to a spatial power growth of 2.3dB/cm. Hence the wave would increase by ~70dB in going once around the interaction space. We note that this growth rate is larger in magnitude than the growth rate[9] of the space-charge, surface wave instability discussed earlier.

In conclusion, we have described the basic concepts of a novel source of coherent electromagnetic radiation capable of generating waves in the millimeter and submillimeter wavelength ranges. It employs the compact magnetron geometry with a superimposed periodic wiggler magnetic field which replaces the periodic assembly of resonators in conventional magnetrons. The instability mechanism is that of the high gain free electron laser operating in the high density collective regime. However, detailed computations of the dispersion relation that take into account finite geometry, the dc electric space-charge field and the velocity shear in the Brillouin equilibrium must be undertaken before a full theoretical assessment of the rippled-field magnetron can be made. The design of an experimental device is in progress.

ACKNOWLEDGMENTS

This work was supported in part by the Air Force Office of Scientific Research, in part by the Department of the Air Force Aeronautical Systems Division (AFSC), and in part by the National Science Foundation.

Table 1. Summary of Operating Parameters of a Rippled Field Magnetron.

r_a	=	4.64cm
r_c	=	4.14cm
V	=	1.022MV
B_{0z}	=	10.32kG
B_{0c}	=	10.20kG
$B_z(x^*)$	=	13.54kG
$E_x(x^*)$	=	3.60×10^{6}V/cm
$v_y(x^*)/c$	=	0.885
x^*/d	=	0.758
$\omega_p(x^*)$	=	$1.62\times10^{11}\text{sec}^{-1}$
$\Omega(x^*)$	=	$2.38\times10^{11}\text{sec}^{-1}$
B_w	=	2.28kG
N	=	26
ω_r	=	$1.46\times10^{12}\text{sec}^{-1}$
ω_i	=	$8.11\times10^{9}\text{sec}^{-1}$

REFERENCES

1. Microwave Magnetrons, edited by G.B. Collins (McGraw-Hill, New York, 1948); also Crossed-Field Microwave Devices, edited by E. Okress (Academic, New York, 1961.)

2. G. Bekefi and T.J. Orzechowski, Phys. Rev. Lett. 37, 379 (1976); A. Palevsky and G. Bekefi, Phys. Fluids 22, 986 (1979); A. Palevsky, G. Bekefi, and A.T. Drobot, J. Appl. Phys. 52, 4938 (1981).

3. T.J. Orzechowski and G. Bekefi, Phys. Fluids 19, 43 (1976); 22, 978 (1979) and references therein.

4. A. Gover and A. Yariv, Appl. Physics 16, 121 (1978).

5. N.M. Kroll and W. A. McMullin, Phys. Rev. A17, 300 (1978); P. Sprangle and R.A. Smith, Phys. Rev. A21, 293 (1980).

6. O. Buneman, in Crossed-Field Microwave Devices, edited by E. Okress (Academic, New York, 1961), Vol. 1, p. 209.

7. E. Ott and R.V. Lovelace, Appl. Phys Lett. 27, 378 (1975).

8. K. Halbach, Lawrence Berkeley Laboratory, University of California, Accelerator and Fusion Research Division Report No. LBL 11393, August 1980.

9. J. Swegle and E. Ott, Phys. Rev. Lett. 46, 929 (1981); Phys. Fluids 24, 1821 (1981).

10. G.G. Macfarlane and H.G. Hay, Proc. Phys. Soc. B 63, 409 (1950).

11. O. Buneman, R.H. Levy, and L.M. Linson, J. Appl. Phys. 37, 3203 (1966).

FIGURE CAPTIONS

Fig. 1. Schematic diagram of a rippled-field magnetron.

Fig. 2. The planar version of the rippled-field magnetron.

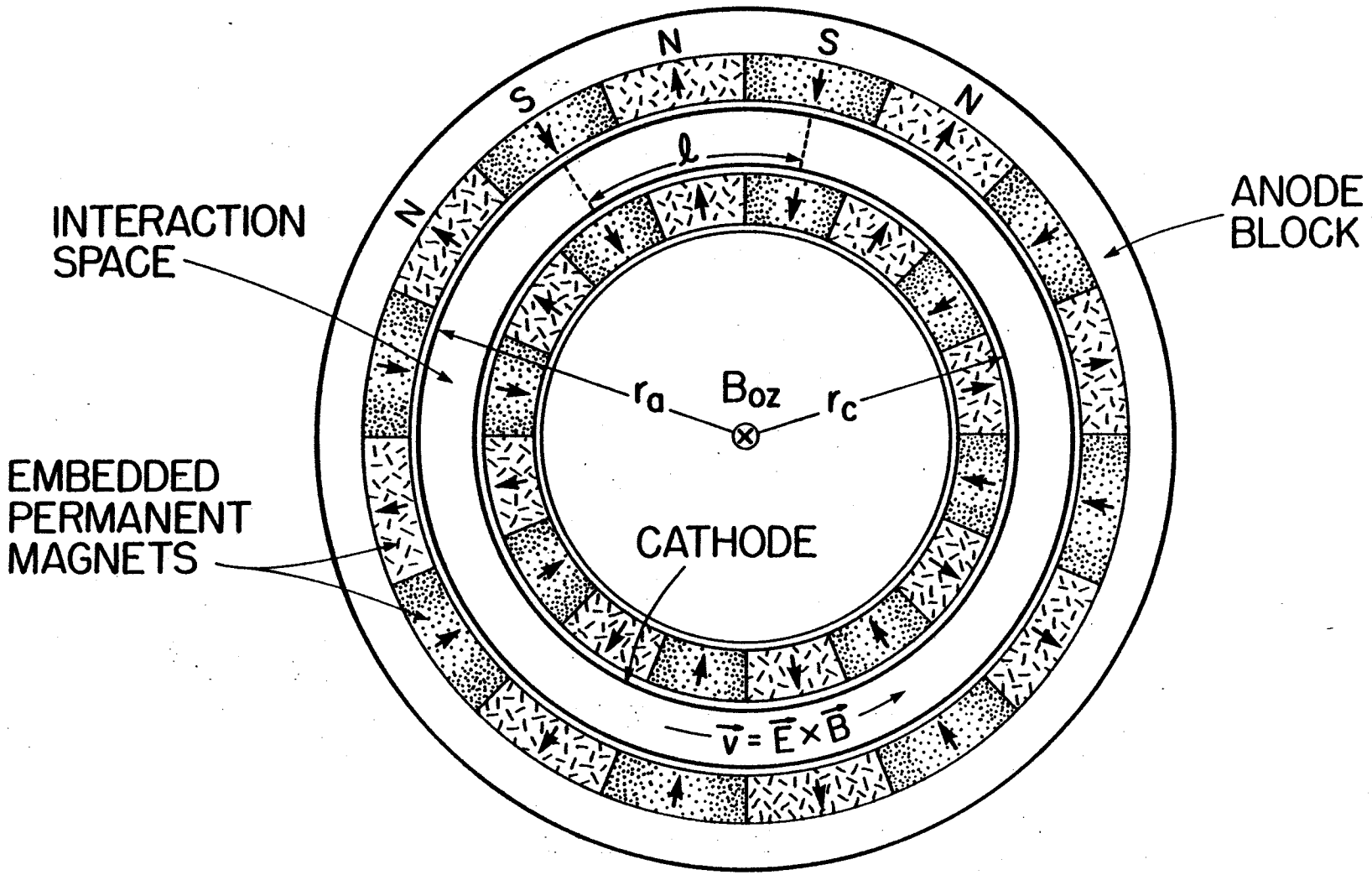
N
S
N
S
N
S
ℓ
INTERACTION SPACE
ANODE BLOCK
r_a
B_{oz}
r_c
EMBEDDED PERMANENT MAGNETS
CATHODE
$\vec{v} = \vec{E} \times \vec{B}$

Fig. 1
Bekefi

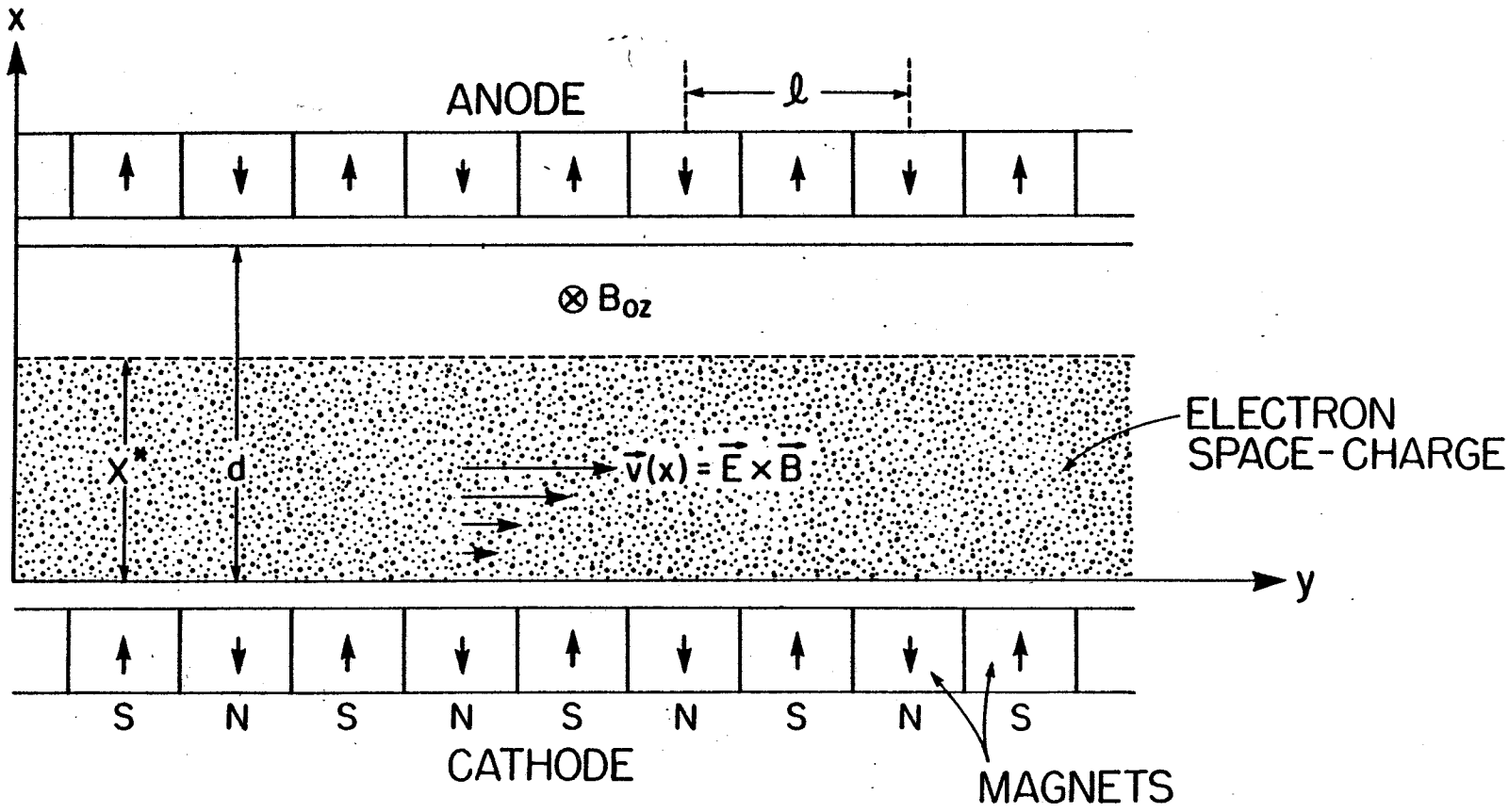
x
ANODE
ℓ
⊗ B0z
X*
d
v(x) = E × B
ELECTRON
SPACE-CHARGE
y
S N S N S N S N S
CATHODE
MAGNETS

Fig. 2
Bekefi